

Random Forests as Statistical Procedures: Design, Variance, and Dependence

Nathaniel S. O'Connell

Department of Biostatistics and Data Science, Wake Forest University School of Medicine
Winston-Salem, NC, United States
nathaniel.oconnell@wfusm.edu

Abstract

Random forests are widely used prediction procedures, yet are typically described algorithmically rather than as statistical designs acting on a fixed dataset. We develop a finite-sample, design-based formulation of random forests in which each tree is an explicit randomized conditional regression function. This perspective yields an exact variance identity for the forest predictor that separates finite-aggregation variability from a structural dependence term that persists even under infinite aggregation. We further decompose both single-tree dispersion and inter-tree covariance using the laws of total variance and covariance, isolating two fundamental design mechanisms—reuse of training observations and alignment of data-adaptive partitions. These mechanisms induce a strict covariance floor, demonstrating that predictive variability cannot be eliminated by increasing the number of trees alone. The resulting framework clarifies how resampling, feature-level randomization, and split selection govern resolution, tree variability, and dependence, and establishes random forests as explicit finite-sample statistical designs whose behavior is determined by their underlying randomized construction.

Keywords: Random Forest; Randomized Design; Variance; Covariance; Resolution

1 Introduction

1.1 Existing theory and its limitations

Since their introduction by Breiman (2001), Random Forests have been among the most widely used modeling frameworks for prediction, adopted across a wide range of scientific domains, and widely regarded as providing strong predictive performance, stability, and robustness to tuning (Hastie et al., 2009). Despite this widespread use, random forests are most often presented as algorithms—ensembles of randomized decision trees motivated empirically or through large-sample arguments—rather than as finite-sample statistical procedures defined by an explicit randomization scheme.

This algorithmic framing has shaped much of the theoretical literature. Early work studied their consistency properties (Breiman, 2004), while subsequent work established consistency and rates of convergence under structural assumptions on splitting rules and feature distributions (Biau et al., 2008; Biau, 2012; Scornet et al., 2015; Biau and Scornet, 2016). Complementary work showed that random forest predictors can be represented as adaptive nearest-neighbor or weighted regression estimators, with predictions expressed as weighted averages of observed responses and weights induced by recursive partitioning (Lin and Jeon, 2006; Biau and Devroye, 2010; Meinshausen, 2006; Athey et al., 2019). These results reveal an underlying statistical structure, but do not provide a finite-sample characterization of how predictive variability and dependence arise from the forest-generating randomization itself.

More recent work has treated random forests as statistical estimators and developed asymptotic distributional theory using U-statistic, V-statistic, and influence-function representations (Mentch and Hooker, 2016; Zhou et al., 2021; Wager and Athey, 2018). These approaches characterize sampling variability under repeated data generation, but they do not analyze the procedural variability induced by the randomization used to construct the forest for a fixed observed dataset. More generally, the variability of a random forest predictor reflects two distinct sources of randomness: sampling variability arising from repeated draws of the dataset, and procedural variability induced by the ‘randomness’ of the Random Forest itself. Existing theory primarily addresses the former. Related work on variance estimation (Xu et al., 2024) conditions on the forest construction mechanism and yields asymptotically valid estimators under repeated sampling, but likewise does not provide an exact finite-sample decomposition of the variability induced by the tree-generating design.

At the same time, it has long been recognized that correlation between ensemble members limits the extent to which aggregation can reduce predictive variability. This phenomenon appears prominently in the literature on bagging and ensemble learning (Breiman, 1996; Dietterich, 2000; Bühlmann and Yu, 2002; Kuncheva and Whitaker, 2003; Brown et al., 2005). More recent work emphasizes that additional sources of randomization can improve predictive performance by weakening dependence between trees, even when individual trees become more variable (Mentch and Zhou, 2020, 2022; Liu and Mazumder, 2025). Other analyses study algorithmic variance and convergence of randomized ensembles conditional on the training data (Lopes et al., 2019a,b). These contributions document the presence and consequences of dependence, but they do not yield an explicit finite-sample decomposition of predictive variability or isolate the structural sources of dependence induced by distinct design choices.

1.2 A design-based perspective

Recent work has broadly synthesized how Random Forests work as adaptive smoothers Curth et al. (2024). In this paper, we approach Random Forests through a difference lens – we define random forests as finite-sample statistical procedures generated by an explicit randomized design acting on a fixed observed dataset $\mathcal{D}_n = \{(X_i, Y_i)\}_{i=1}^n$. Each tree is constructed by randomized operations (e.g. observation selection (Breiman, 1996), random subspace selection for candidate splits (Ho, 1998), and stochastic split choice), that determine how the observed outcomes are combined to form predictions. All variability in the forest predictor is induced by this tree-generating design; the data \mathcal{D}_n are treated as fixed and no probability model is imposed on the covariates or outcomes. All results are exact at fixed n .

When the dataset itself is viewed as random under repeated sampling, the unconditional variability of the forest predictor decomposes into a sampling component and a design component. The sampling component reflects instability of the induced infinite-forest target (the deterministic limit of the forest predictor as the number of trees goes to infinity) across datasets and, under standard stability conditions, decreases at the $O(n^{-1})$ rate. By contrast, the design component captures finite-sample variability introduced by the forest’s randomized construction acting on a fixed dataset and depends explicitly on aggregation, subsampling, and partitioning choices. Section 2 formalizes this decomposition and motivates our focus on the design-induced variability that distinguishes random forests as statistical procedures.

Within this framework, we study the random forest predictor itself as a statistical procedure induced by a randomized design. Although resampling-based performance estimates—most notably out-of-bag evaluation—are produced as a byproduct of the forest construction, they correspond to distinct estimands and should not be conflated with the predictor itself. Out-of-bag evaluation is a form of internal cross-validation targeting predictive risk, whereas our analysis concerns the behavior of the fitted forest predictor itself at a fixed prediction point. This distinction parallels classical regression analysis, in which one studies the properties of a fitted generalized linear model independently of how cross-validation is used to assess its predictive performance.

We show that random forests can be represented as averages of randomized conditional regression functions. Each tree induces a data-adaptive local regression, expressible as a weighted average of observed responses with weights determined by the induced partition of the feature space. Averaging these randomized regressions yields a natural design-based target for the forest predictor. Within this formulation, we derive an exact finite-sample variance identity that separates aggregation variability from a structural dependence component that persists under infinite aggregation, and we show how common forest hyperparameters govern resolution, single-tree variability, and structural dependence.

2 Random Forests as Statistical Procedures

2.1 Variance decomposition and scope

We distinguish two sources of variability in random forest prediction: algorithmic variability induced by the forest-generating randomization acting on a fixed realized dataset, and sampling variability arising from repeated draws of the dataset from an underlying population.

Let \mathcal{D}_n^* denote a generic sample of size n from the population, and let $\hat{f}_B(x; \mathcal{D}, \theta)$ denote the B -tree forest predictor constructed from dataset \mathcal{D} using design randomization θ . The unconditional variance across repeated datasets and forest constructions decomposes by the law of total variance as

$$\text{Var}(\hat{f}_B(x; \mathcal{D}_n^*, \theta)) = \mathbb{E}[\text{Var}(\hat{f}_B(x; \mathcal{D}_n^*, \theta) | \mathcal{D}_n^*)] + \text{Var}(\mathbb{E}[\hat{f}_B(x; \mathcal{D}_n^*, \theta) | \mathcal{D}_n^*]).$$

This decomposition is standard – see for example a similar representatin in (Hastie et al., 2009) and (Curth et al., 2024) – where it is used to separate sampling variance from algorithmic variance in the conventional bias-variance framework. Our use of this identity differs in purpose. We take the next step and condition on the realized dataset \mathcal{D}_n^* . In doing so, we isolate the first term as the design-induced variability arising from the random forest applied to a fixed dataset, while the second captures sampling variability across repeated datasets. Under standard stability conditions, the sampling component is generically $O(n^{-1})$, reflecting conventional large-sample behavior; a derivation based on asymptotic linearity is given in Appendix A, with related results in Menth and Hooker (2016); Wager and Athey (2018).

Unlike sampling variability, the design-induced variability persists at finite sample sizes and depends explicitly on forest hyperparameters governing aggregation, subsampling, and partitioning resolution. These choices control single-tree variability, the strength of dependence between trees, and the extent to which aggregation can reduce variance. Accordingly, for the remainder of this paper we fix the realized dataset \mathcal{D}_n and focus on an exact finite-sample analysis of the design-induced variability $\text{Var}(\hat{f}_B(x; \mathcal{D}_n, \theta))$. All probabilistic quantities are therefore evaluated under the design-induced distribution conditional on a fixed \mathcal{D}_n ; for notational simplicity we suppress the subscript \mathcal{D}_n on $\text{Var}(\cdot)$, $\text{Cov}(\cdot)$, and $E(\cdot)$.

2.2 Tree-level randomized regression functions

We formalize a single tree as a randomized prediction rule acting on a fixed observed dataset $\mathcal{D}_n = \{(X_i, Y_i)\}_{i=1}^n$, with $X_i \in \mathcal{X} \subset \mathbb{R}^p$ and $Y_i \in \mathbb{R}$. A tree is generated by applying a randomized recursive partitioning algorithm to \mathcal{D}_n , incorporating operations such as observation selection, random subspace selection for candidate splits, and stochastic split choice. A particular realization of this algorithmic randomization is indexed by θ , and the resulting predictor is denoted by T_θ . For fixed θ , the tree and its induced prediction rule are deterministic functions of \mathcal{D}_n .

For a prediction point $x \in \mathcal{X}$, the tree-generating mechanism θ induces a random averaging set

$$A_\theta(x) := \{i \in \{1, \dots, n\} : X_i \text{ is routed with } x \text{ under tree } \theta\},$$

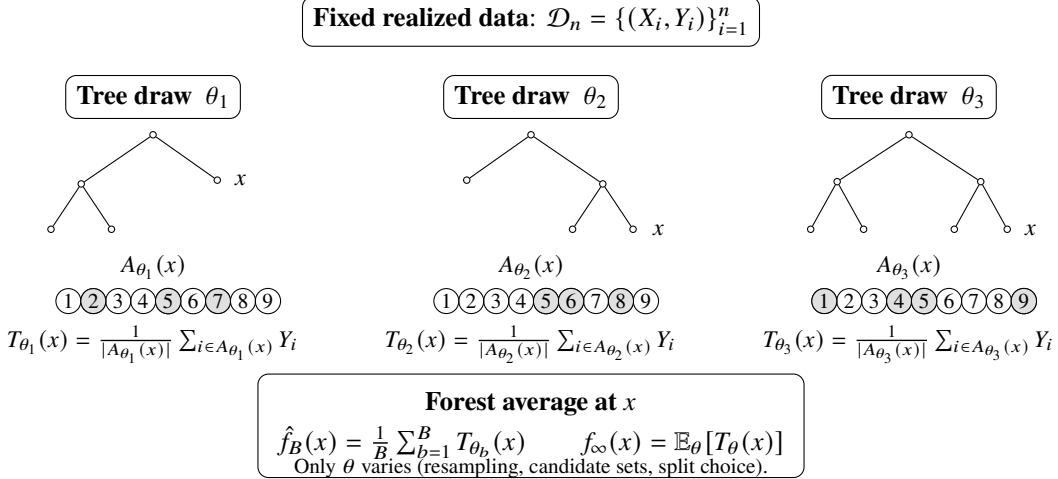


Figure 1: **Random forests as randomized local averaging on fixed outcomes.** \mathcal{D}_n are fixed. Independent draws of the tree-generating design $\theta_1, \theta_2, \theta_3$ induce realized tree structures and tree specific terminal-node membership sets $A_{\theta_b}(x)$ for prediction point x . Each tree prediction is the average over indexed outcomes in its membership set, and averaging over independent draws yields $\hat{f}_B(x)$ and $f_\infty(x)$.

consisting of the training observations grouped with x in the terminal node reached by x . The set $A_\theta(x)$ is the primitive object governing the tree-level prediction at x and depends on all sources of algorithmic randomness. Define the terminal membership indicator

$$M_{i,\theta}(x) := \mathbf{1}\{i \in A_\theta(x)\},$$

which records whether observation i contributes to the prediction at x in tree θ . Under squared-error loss, the tree prediction at x is the CART terminal-node estimate (Breiman et al., 1984),

$$T_\theta(x) = \frac{1}{|A_\theta(x)|} \sum_{i \in A_\theta(x)} Y_i = \sum_{i=1}^n W_i(x; \theta) Y_i, \quad W_i(x; \theta) := \frac{M_{i,\theta}(x)}{|A_\theta(x)|}.$$

The weights $W_i(x; \theta)$ are normalized membership indicators derived entirely from the averaging set $A_\theta(x)$ and introduce no additional randomness beyond the grouping induced by the tree. As θ varies under the tree-generating mechanism, the prediction $T_\theta(x)$ varies solely through the induced averaging set, equivalently through the collection of indicators $\{M_{i,\theta}(x)\}_{i=1}^n$. Although the observed outcomes $Y_{1:n}$ are treated as fixed, $A_\theta(x)$ depends on them because split selection optimizes impurity criteria computed from the resampled outcomes determined by θ .

Representations of random forests as adaptive weighted averages of the training responses are well established (Lin and Jeon, 2006; Biau and Devroye, 2010; Scornet et al., 2015) and underlie extensions such as quantile regression forests (Meinshausen, 2006). Our contribution is not the algebraic form itself, but the probabilistic framing: we treat the random weight vector $W(x; \theta)$ as the primary random object in the design-based probability space. In this view, the infinite-aggregation predictor arises as the expectation of this random weight vector, and properties such as resolution and structural dependence are governed by its distribution rather than by the fitted tree viewed as a fixed estimator.

2.3 The forest predictor and its design-based target

A random forest predictor is a Monte Carlo average of randomized tree-level prediction rules. Let $\{T_{\theta_b}\}_{b=1}^B$ denote B independent realizations of the tree-generating mechanism described in Section 2.2. The finite

forest predictor is

$$\hat{f}_B(x) = \frac{1}{B} \sum_{b=1}^B T_{\theta_b}(x) = \sum_{i=1}^n \hat{W}_i^{(B)}(x) Y_i, \quad \hat{W}_i^{(B)}(x) := \frac{1}{B} \sum_{b=1}^B W_i(x; \theta_b).$$

The aggregation level B controls only the amount of Monte Carlo averaging and does not alter the distribution of the underlying tree-level rule. Let θ denote a generic draw from the tree-generating mechanism and define the infinite-aggregation target

$$f_\infty(x) = \mathbb{E}[T_\theta(x)],$$

where the expectation is taken with respect to the tree-generating randomization acting on the fixed dataset \mathcal{D}_n . This quantity is fully determined by the forest design and the observed data and represents the deterministic prediction induced by the procedure under infinite aggregation. The finite forest predictor $\hat{f}_B(x)$ is a Monte Carlo approximation to $f_\infty(x)$, satisfying $\mathbb{E}[\hat{f}_B(x)] = f_\infty(x)$. Finite forests fluctuate around this target due to limited aggregation, while structural dependence between tree-level prediction rules induces a non-zero covariance component as $B \rightarrow \infty$. The variance analysis that follows makes this separation explicit.

3 Variance of Random Forest Predictors

3.1 Finite-sample variance identity

We now characterize the finite-sample variance of the random forest predictor $\hat{f}_B(x)$ under the design-induced distribution. Recall that $\hat{f}_B(x)$ is the average of B independent realizations $T_{\theta_b}(x)$ of the randomized tree-level prediction rule $T_\theta(x)$ acting on the fixed dataset \mathcal{D}_n . Define

$$\sigma_T^2(x) = \text{Var}(T_\theta(x)), \quad C_T(x) = \text{Cov}(T_\theta(x), T_{\theta'}(x)),$$

where θ and θ' denote independent draws from the tree-generating mechanism. Although trees are generated independently, the resulting predictions need not be independent, because each tree acts on the same realized dataset through design-induced random averaging sets. This dependence is captured by the covariance term $C_T(x)$.

Theorem 1 (Finite-sample variance identity for random forests). *For any $B \geq 1$,*

$$\text{Var}(\hat{f}_B(x)) = \frac{1}{B} \sigma_T^2(x) + \frac{B-1}{B} C_T(x).$$

Proof. Write $\hat{f}_B(x) = B^{-1} \sum_{b=1}^B T_{\theta_b}(x)$. Then

$$\text{Var}(\hat{f}_B(x)) = \frac{1}{B^2} \text{Var}\left(\sum_{b=1}^B T_{\theta_b}(x)\right) = \frac{1}{B^2} \sum_{b=1}^B \sum_{b'=1}^B \text{Cov}(T_{\theta_b}(x), T_{\theta_{b'}}(x)).$$

By exchangeability of the tree-generating mechanism, $\text{Cov}(T_{\theta_b}(x), T_{\theta_{b'}}(x)) = \sigma_T^2(x)$ for all b and $\text{Cov}(T_{\theta_b}(x), T_{\theta_{b'}}(x)) = C_T(x)$ for all $b \neq b'$. Therefore

$$\text{Var}(\hat{f}_B(x)) = \frac{1}{B^2} \left(B \sigma_T^2(x) + B(B-1) C_T(x) \right) = \frac{1}{B} \sigma_T^2(x) + \frac{B-1}{B} C_T(x).$$

□

This identity separates variability due to finite aggregation, represented by $\sigma_T^2(x)/B$, from structural dependence induced by the design through the joint behavior of tree-level averaging sets, represented by $C_T(x)$. The result follows directly from exchangeability of the tree-level prediction rules under the tree-generating mechanism.

3.2 Decomposing the single-tree variance

We now decompose the single-tree variance term $\sigma_T^2(x)$ appearing in Theorem 1. Let $\mathcal{I}_\theta = (I_{\theta,1}, \dots, I_{\theta,n})$ denote the resampling indicators for the tree indexed by θ , where $I_{\theta,i} = 1$ if observation i is exposed to the tree construction and $I_{\theta,i} = 0$ otherwise. For a fixed prediction point x , the resampling indicators determine which observations are eligible to appear in the random averaging set $A_\theta(x)$, while the remaining algorithmic randomness—such as feature subsampling and split selection—determines how x is grouped with those observations. Conditioning on \mathcal{I}_θ and applying the law of total variance yields

$$\sigma_T^2(x) = \mathbb{E}[\text{Var}(T_\theta(x) \mid \mathcal{I}_\theta)] + \text{Var}(\mathbb{E}[T_\theta(x) \mid \mathcal{I}_\theta]). \quad (1)$$

The first term in (1) captures variability arising from random splitting decisions after the resampling pattern is fixed, while the second captures variability induced by changes in the resampling realization itself, which alter which observations are eligible to be grouped with x . We now focus on the first component and examine how randomness in local grouping contributes to single-tree variability.

3.3 Decomposing the within-resample variance term

We now refine the first term in (1), corresponding to variability induced by random splitting decisions after the resampling pattern is fixed. Define

$$V_{\text{in}}(x) = \mathbb{E}[\text{Var}(T_\theta(x) \mid \mathcal{I}_\theta)].$$

Conceptually, $V_{\text{in}}(x)$ measures how sensitive the prediction at x is to the particular way the tree is grown, holding fixed which observations are available to it. Even with the same resampled data, different choices of candidate split variables, cutpoints, or tie-breaking can route x into different terminal nodes and therefore group it with different subsets of observations. Under a fixed resampling pattern, the remaining tree-level randomization affects $T_\theta(x)$ only through the induced averaging set $A_\theta(x)$. Conditioning on $A_\theta(x)$ therefore fixes the local grouping used to form the prediction at x . Applying the law of total variance with $A_\theta(x)$ as the intermediate conditioning object yields

$$V_{\text{in}}(x) = \mathbb{E}[\text{Var}(T_\theta(x) \mid \mathcal{I}_\theta, A_\theta(x))] + \mathbb{E}[\text{Var}(\mathbb{E}[T_\theta(x) \mid \mathcal{I}_\theta, A_\theta(x)] \mid \mathcal{I}_\theta)]. \quad (2)$$

The first term in (2) does not represent additional algorithmic randomness. Once both the resampling pattern and the averaging set at x are fixed, the tree prediction is deterministic. This component reflects how intrinsic outcome dispersion at the observations grouped with x appears in the value of a fixed local average. Conditional on $(\mathcal{I}_\theta, A_\theta(x))$,

$$\text{Var}(T_\theta(x) \mid \mathcal{I}_\theta, A_\theta(x)) = \sum_{i=1}^n W_i(x; \theta)^2 \text{Var}(Y_i \mid \mathcal{I}_\theta, A_\theta(x)) + C_\theta(x),$$

where $C_\theta(x)$ collects cross-unit covariance terms and is zero under conditional independence across observational units. Conditioning on $(\mathcal{I}_\theta, A_\theta(x))$ fixes only how observations are grouped with x and does not alter their outcome-generating behavior, so $\text{Var}(Y_i \mid \mathcal{I}_\theta, A_\theta(x)) = \text{Var}(Y \mid X = X_i)$. Writing this deterministic quantity as σ_i^2 ,

$$\mathbb{E}[\text{Var}(T_\theta(x) \mid \mathcal{I}_\theta, A_\theta(x))] = \sum_{i=1}^n \sigma_i^2 \mathbb{E}[W_i(x; \theta)^2].$$

This term captures the intrinsic statistical variability of the averaging rule itself: how outcome noise at contributing observations propagates through a fixed local average. The quantity $\sigma_i^2 = \text{Var}(Y \mid X = X_i)$ is

a population-level conditional second moment that characterizes the intrinsic variability of outcomes at the covariate location X_i . It is not a parameter of the randomized design and is not a source of variability under the design-based distribution; rather, it enters as a fixed scalar when the design-induced variance is expanded at a known averaging set. In this sense, σ_i^2 plays the same role as the observed outcomes Y_i themselves: it is a fixed attribute of the statistical environment in which the design operates. The decomposition holds for any values of σ_i^2 and does not require their estimation.

The second term in (2) captures variability arising purely from randomness in the induced averaging set. Even with the resampling pattern fixed, different realizations of the remaining tree-level randomization can induce different sets $A_\theta(x)$ and hence different local groupings of observations around x . Because $\mathbb{E}[T_\theta(x) | \mathcal{I}_\theta, A_\theta(x)] = \sum_{i=1}^n W_i(x; \theta) Y_i$, where the weights are deterministic functions of the averaging set, this component measures variability in the prediction at x induced by randomness in the grouping itself, holding the observed outcomes fixed:

$$\mathbb{E}\left[\text{Var}\left(\sum_{i=1}^n W_i(x; \theta) Y_i \mid \mathcal{I}_\theta\right)\right].$$

It is zero if and only if the averaging set $A_\theta(x)$ is almost surely constant given \mathcal{I}_θ . This term therefore reflects instability in how the tree-growing procedure defines local neighborhoods around x : different partitions lead to different groupings and hence to different predictions, even when the available data are the same.

Together, the two components describe how unstable a single tree's prediction at x can be even when the same resampled data are used: the first term captures intrinsic noise propagation through a fixed averaging rule, while the second captures sensitivity to how that rule is selected.

3.4 Decomposing the resampling component

We next interpret the second term in (1),

$$V_{\text{out}}(x) := \text{Var}(\mathbb{E}[T_\theta(x) | \mathcal{I}_\theta]),$$

which captures variability induced by the resampling design across trees. This component measures how the *average* prediction at x changes across resampling realizations, before accounting for any additional variability from the remaining tree-level randomization. Conditioning on the resampling indicators and using the weighted representation of the tree predictor,

$$\mathbb{E}[T_\theta(x) | \mathcal{I}_\theta] = \sum_{i=1}^n \bar{W}_i(x; \mathcal{I}_\theta) Y_i, \quad \bar{W}_i(x; \mathcal{I}_\theta) := \mathbb{E}[W_i(x; \theta) | \mathcal{I}_\theta],$$

where $\bar{W}_i(x; \mathcal{I}_\theta)$ is the expected weight assigned to observation i at x under the remaining tree-level randomization, given the resampling realization. With this notation,

$$V_{\text{out}}(x) = \text{Var}\left(\sum_{i=1}^n \bar{W}_i(x; \mathcal{I}_\theta) Y_i\right).$$

Conceptually, $V_{\text{out}}(x)$ isolates the effect of resampling on prediction. Different resampling realizations \mathcal{I}_θ change which observations are exposed to the tree, which in turn alters the distribution of the induced averaging set $A_\theta(x)$ and hence shifts the *expected* local averaging rule $\bar{W}(x; \mathcal{I}_\theta)$. Unlike $V_{\text{in}}(x)$, which reflects instability in how a given resampled dataset is locally partitioned, $V_{\text{out}}(x)$ reflects variability arising from changes in which observations are even eligible to contribute to the prediction at x .

4 Decomposing the Covariance Structure

4.1 Law of Total Covariance Decomposition

We now examine the covariance term $C_T(x)$ appearing in Theorem 1. From the finite-sample variance identity, $C_T(x)$ is the limiting contribution to predictive variability as $B \rightarrow \infty$, representing irreducible dependence between tree-level prediction rules induced by the forest design at fixed sample size. Although the trees indexed by θ and θ' are generated independently, their predictions at x are generally dependent because both act on the same fixed dataset through randomized grouping mechanisms. To isolate the sources of this dependence, we condition on the resampling indicators \mathcal{I}_θ and $\mathcal{I}_{\theta'}$, which determine which observations are exposed to each tree. Conditional on these indicators, any remaining dependence reflects how the forest construction induces related prediction rules at x under independent tree generation.

Applying the law of total covariance with respect to the resampling indicators yields

$$C_T(x) = \mathbb{E}[\text{Cov}(T_\theta(x), T_{\theta'}(x) \mid \mathcal{I}_\theta, \mathcal{I}_{\theta'})] + \text{Cov}(\mathbb{E}[T_\theta(x) \mid \mathcal{I}_\theta], \mathbb{E}[T_{\theta'}(x) \mid \mathcal{I}_{\theta'}]). \quad (3)$$

Because the two trees are generated independently, $\mathcal{I}_{\theta'}$ carries no information about $T_\theta(x)$ beyond \mathcal{I}_θ , and likewise with roles reversed; we therefore suppress redundant conditioning arguments implied by independence.

The two terms in (3) correspond to distinct design mechanisms. The first term captures dependence arising from joint inclusion of observations in the averaging sets $A_\theta(x)$ and $A_{\theta'}(x)$, whereby the same outcomes receive positive weight in both trees. The second term captures dependence arising from alignment of the induced prediction rules at x : even when the averaging sets are disjoint, independently generated trees may induce similar local averaging behavior after conditioning on their respective resampling realizations.

This decomposition is exact at fixed sample size. Resampling schemes govern the first term through joint inclusion probabilities in the averaging sets, while feature-level randomization and split selection govern the second term through stability or alignment of the induced grouping mechanism around x . The following subsections analyze these components in turn.

4.2 Covariance Induced by Shared Training Observations

We analyze first the leading term $\mathbb{E}[\text{Cov}(T_\theta(x), T_{\theta'}(x) \mid \mathcal{I}_\theta, \mathcal{I}_{\theta'})]$, which captures dependence arising from reuse of the same training observations in the predictions at x . This mechanism is present whenever the same observation receives nonzero weight in both trees at x . Joint inclusion in the resampling realizations is necessary but not sufficient; the observation must also lie in the terminal region containing x in both trees.

Using the weighted representation $T_\theta(x) = \sum_{i=1}^n W_i(x; \theta) Y_i$ and conditioning on $(\mathcal{I}_\theta, \mathcal{I}_{\theta'})$, the covariance expands as

$$\begin{aligned} \text{Cov}(T_\theta(x), T_{\theta'}(x) \mid \mathcal{I}_\theta, \mathcal{I}_{\theta'}) &= \text{Cov}\left(\sum_{i=1}^n W_i(x; \theta) Y_i, \sum_{j=1}^n W_j(x; \theta') Y_j \mid \mathcal{I}_\theta, \mathcal{I}_{\theta'}\right) \\ &= \sum_{i=1}^n \sum_{j=1}^n W_i(x; \theta) W_j(x; \theta') \text{Cov}(Y_i, Y_j \mid X_i, X_j). \end{aligned}$$

Under conditional independence of outcomes across observational units given the fixed design points, $\text{Cov}(Y_i, Y_j \mid X_i, X_j) = 0$ for $i \neq j$, so the double sum reduces to

$$\text{Cov}(T_\theta(x), T_{\theta'}(x) \mid \mathcal{I}_\theta, \mathcal{I}_{\theta'}) = \sum_{i=1}^n W_i(x; \theta) W_i(x; \theta') \sigma_i^2.$$

Where $\sigma_i^2 = \text{Var}(Y|X = X_i)$ as defined in Section 3.3. Taking expectations over the tree-generating randomization yields

$$\mathbb{E}[\text{Cov}(T_\theta(x), T_{\theta'}(x) | \mathcal{I}_\theta, \mathcal{I}_{\theta'})] = \sum_{i=1}^n \mathbb{E}[W_i(x; \theta) W_i(x; \theta')] \sigma_i^2.$$

The joint weight factor can be decomposed as

$$\mathbb{E}[W_i(x; \theta) W_i(x; \theta')] = \mathbb{P}(I_{\theta,i} = 1, I_{\theta',i} = 1) \mathbb{E}[W_i(x; \theta) W_i(x; \theta') | I_{\theta,i} = I_{\theta',i} = 1],$$

separating joint inclusion under the resampling scheme from the conditional allocation of weight induced by the local partitions. This contribution reflects dependence induced purely by repeated reuse of the same observations in the predictions at x . It persists regardless of whether the induced partitions agree across trees, and is identically zero only when the resampling design assigns zero probability to joint inclusion of any observation across trees.

4.3 Covariance Induced by Partition Alignment

We now analyze the second term in (3),

$$\text{Cov}(\mathbb{E}[T_\theta(x) | \mathcal{I}_\theta], \mathbb{E}[T_{\theta'}(x) | \mathcal{I}_{\theta'}]),$$

which captures dependence arising from alignment of the induced local geometry around x across independently generated trees. This mechanism does not require any observation to receive positive weight in both trees at x in a given realization. Instead, it arises when distinct trees, potentially trained on disjoint exposed subsets, induce the same (or very similar) terminal region containing x and therefore apply similar local averaging rules. Concretely, two trees trained on different observations may split on the same variables in the approximately the same order at similar thresholds in a neighborhood of x ; in that case x is routed into essentially the same geometric terminal node, and each tree averages outcomes from the same covariate-defined subpopulation even if the contributing training observations are disjoint.

To formalize this, let $R_\theta(x) \subset \mathcal{X}$ denote the terminal region containing x under tree draw θ . Because only observations exposed to the tree can be routed, the averaging set defined in Section 2.2 can be written equivalently as

$$A_\theta(x) = \{i : I_{\theta,i} = 1, X_i \in R_\theta(x)\}, \quad W_i(x; \theta) = \frac{\mathbf{1}\{I_{\theta,i} = 1\} \mathbf{1}\{X_i \in R_\theta(x)\}}{|A_\theta(x)|}.$$

Thus, $T_\theta(x)$ is a local average over exposed outcomes in the covariate-defined region $R_\theta(x)$. When independent trees induce similar regions $R_\theta(x)$ and $R_{\theta'}(x)$, they average different observations drawn from essentially the same local subpopulation determined by those split conditions, producing dependence through aligned local geometry rather than shared outcomes.

Conditional on the resampling indicators \mathcal{I}_θ , the remaining randomness in $T_\theta(x)$ arises from feature subsampling and split selection, which determine the realized region $R_\theta(x)$ and hence the induced averaging set. Averaging over this remaining randomness induces the resampling-conditional prediction rule

$$Z_\theta(x) := \mathbb{E}[T_\theta(x) | \mathcal{I}_\theta], \quad Z_{\theta'}(x) = \mathbb{E}[T_{\theta'}(x) | \mathcal{I}_{\theta'}].$$

Define the resampling-conditional mean weights

$$\bar{W}_i(x; \mathcal{I}_\theta) := \mathbb{E}[W_i(x; \theta) | \mathcal{I}_\theta], \quad i = 1, \dots, n,$$

so that

$$Z_\theta(x) = \sum_{i=1}^n \bar{W}_i(x; \mathcal{I}_\theta) Y_i, \quad Z_{\theta'}(x) = \sum_{i=1}^n \bar{W}_i(x; \mathcal{I}_{\theta'}) Y_i.$$

The mean weights $\bar{W}_i(x; \mathcal{I}_\theta)$ do not correspond to membership in a single realized terminal region. Rather, they average over the distribution of terminal regions induced by split-level randomization, assigning observation i mass proportional to how frequently it is grouped with x across possible tree realizations. This resampling-conditional mean weight is an intermediate quantity between the realized tree-level weight $W_i(x; \theta)$ and the forest-level expected weight $\mathbb{E}[W_i(x; \theta)]$; its introduction is what makes the alignment mechanism formally identifiable as a distinct component of the covariance structure. In this sense, $\bar{W}_i(x; \mathcal{I}_\theta)$ represents the resampling-conditional local neighborhood around x induced by the procedure.

The alignment component of the covariance is therefore

$$C_{\text{align}}(x) := \text{Cov}(Z_\theta(x), Z_{\theta'}(x)),$$

where the covariance is taken under the design-based distribution induced by the independent resampling indicators $(\mathcal{I}_\theta, \mathcal{I}_{\theta'})$. Expanding yields

$$C_{\text{align}}(x) = \sum_{i=1}^n \sum_{j=1}^n \text{Cov}(Y_i, Y_j \mid X_i, X_j) \mathbb{E}[\bar{W}_i(x; \mathcal{I}_\theta) \bar{W}_j(x; \mathcal{I}_{\theta'})].$$

Under conditional independence of outcomes across observational units given the fixed design points, $\text{Cov}(Y_i, Y_j \mid X_i, X_j) = 0$ for $i \neq j$, and therefore

$$C_{\text{align}}(x) = \sum_{i=1}^n \sigma_i^2 \mathbb{E}[\bar{W}_i(x; \mathcal{I}_\theta) \bar{W}_i(x; \mathcal{I}_{\theta'})]. \quad (4)$$

Expression (4) makes the alignment mechanism explicit in design-based terms. The joint expectation $\mathbb{E}[\bar{W}_i(x; \mathcal{I}_\theta) \bar{W}_i(x; \mathcal{I}_{\theta'})]$ measures whether independent trees tend, on average, to place predictive mass near x on the same local subset of design points after averaging over split-level randomization. When routing near x is stable across tree realizations—so that similar split conditions recur and x repeatedly falls into essentially the same terminal region—the procedure concentrates on a restricted family of local regions in covariate space. The observations populating those regions, though potentially disjoint across trees, are drawn from the same conditional subpopulation defined by the shared partition geometry. Both tree predictions therefore estimate the same conditional mean, yielding positive covariance even in the absence of shared training observations.

4.4 The covariance floor and its strict positivity

The finite-sample variance identity in Theorem 1 implies that the predictive variability of a random forest decomposes into a Monte Carlo component that decreases with the number of trees and a design-induced component that persists under infinite aggregation. In particular,

$$\lim_{B \rightarrow \infty} \text{Var}(\hat{f}_B(x)) = C_T(x),$$

so strict positivity of $C_T(x)$ establishes an irreducible variance floor at fixed sample size induced by the forest design.

Sections 4.2 and 4.3 identified two distinct mechanisms contributing to $C_T(x)$: reuse of training observations in local averages at x , and alignment of the induced local averaging rules across trees. We now show that observation reuse alone is sufficient to guarantee strict positivity of the covariance floor, without invoking any alignment assumptions.

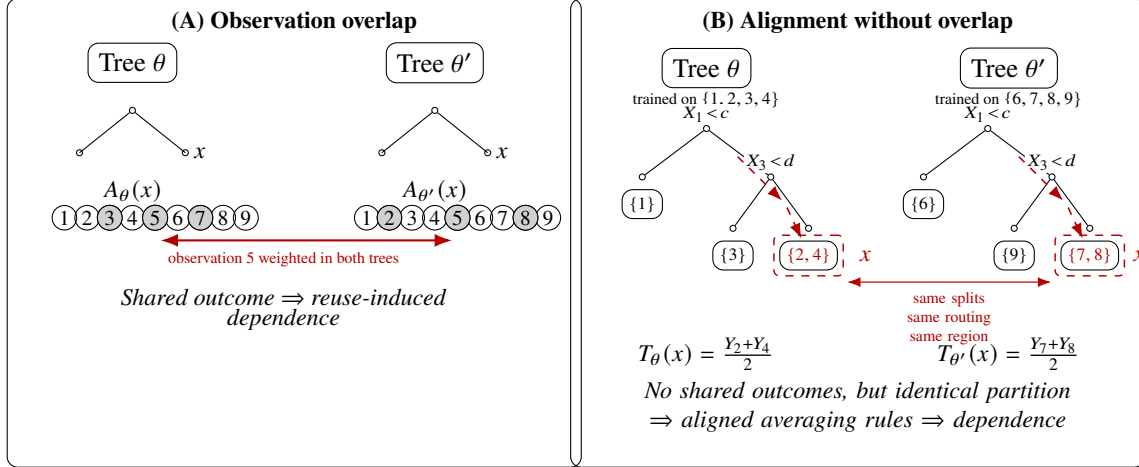


Figure 2: **Two distinct design-induced dependence mechanisms at a fixed prediction point x .** (A) *Observation overlap*: independently generated trees reuse the same outcome (here, Y_5) in their terminal-node averages at x , inducing dependence through shared weighted outcomes. (B) *Partition alignment without overlap*: trees are grown on disjoint training sets ($\{1, 2, 3, 4\}$ and $\{6, 7, 8, 9\}$), yet the covariate geometry near x drives both trees to discover the same splits ($X_1 < c$, then $X_3 < d$). The prediction point x routes identically through both trees (dashed red paths), landing in structurally equivalent terminal regions. The resulting predictions $T_\theta(x)$ and $T_{\theta'}(x)$ average different observations drawn from the same neighborhood of x , producing dependence through aligned local averaging rules rather than shared outcomes.

Theorem 2 (Strict positivity of the covariance floor under observation reuse). *Fix a prediction point x . Suppose there exists an index i^* such that $\sigma_{i^*}^2 > 0$ and $\mathbb{P}(W_{i^*}(x; \theta) > 0) > 0$. Then*

$$C_T(x) > 0, \quad \text{and hence} \quad \lim_{B \rightarrow \infty} \text{Var}(\hat{f}_B(x)) > 0.$$

A proof for Theorem 2 is provided in the Supplemental Materials.

Remark 1 (Design interpretation). Theorem 2 shows that repeated reuse of the same training outcomes in local averages at x is sufficient to induce a strictly positive covariance floor. This effect is governed entirely by the resampling design and persists regardless of the number of trees aggregated. The condition $\mathbb{P}(W_{i^*}(x; \theta) > 0) > 0$ is satisfied by all standard implementations whenever x lies in the support of the design and at least one observation in its neighborhood has positive conditional variance; moreover, the alignment component provides a second, independent nonnegative contribution to the covariance floor that is not required for strict positivity but reinforces it.

4.5 Outcome stability of tree-based predictors

The preceding sections establish that random forest predictors exhibit irreducible dependence across trees induced by the design of the tree-generating mechanism. We now establish a complementary structural property of tree-based predictors: *conditional on a realized tree structure*, predictions at a fixed point are uniformly stable with respect to perturbations of the observed outcomes. This result concerns sensitivity to outcome perturbations holding the induced partition fixed, and is therefore conceptually distinct from the design-induced dependence analyzed above.

Fix a dataset $\mathcal{D}_n = \{(X_i, Y_i)\}_{i=1}^n$ and a prediction point x . Conditional on a realized tree structure, the

induced predictor at x can be written in weighted form as

$$\tilde{f}(x; Y) = \sum_{i=1}^n W_i(x) Y_i,$$

where the weights satisfy $W_i(x) \geq 0$ and $\sum_{i=1}^n W_i(x) = 1$.

Proposition 1 (Uniform outcome stability conditional on tree structure). *Fix a realized tree structure and prediction point x . For any perturbation vector $\delta Y \in \mathbb{R}^n$,*

$$|\tilde{f}(x; Y + \delta Y) - \tilde{f}(x; Y)| \leq \|\delta Y\|_\infty.$$

In particular, conditional on the realized tree structure, the mapping $Y \mapsto \tilde{f}(x; Y)$ is 1-Lipschitz with respect to the ℓ_∞ norm.

Proof. By linearity,

$$\tilde{f}(x; Y + \delta Y) - \tilde{f}(x; Y) = \sum_{i=1}^n W_i(x) \delta Y_i.$$

Because the weights are nonnegative and sum to one,

$$\left| \sum_{i=1}^n W_i(x) \delta Y_i \right| \leq \sum_{i=1}^n W_i(x) |\delta Y_i| \leq \max_{1 \leq i \leq n} |\delta Y_i|.$$

□

Remark 2 (Contrast with coefficient-based predictors). Proposition 1 highlights a structural distinction between tree-based predictors and coefficient-based procedures. For linear and generalized linear models, predictions at a point x depend on the outcomes through fitted coefficients involving an inverse information matrix, so small perturbations in Y can be amplified under near collinearity, with sensitivity governed by the conditioning of the design matrix. By contrast, conditional on their realized structure, tree-based predictors depend on the outcomes only through nonnegative weights summing to one, yielding a uniform ℓ_∞ stability bound that is independent of predictor collinearity or design matrix conditioning. Instability in tree-based methods therefore arises through randomness in the induced partition, not through amplification of outcome noise.

5 Resolution and Structural Error in Random Forests

5.1 The infinite-aggregation target and resolution

Definition 1 (Design-based resolution). Fix a prediction point x and a forest design. The resolution of the infinite-aggregation forest predictor at x is defined by the distribution of the random weight vector $W(x; \theta) = (W_1(x; \theta), \dots, W_n(x; \theta))$ induced by the tree-generating mechanism. Equivalently, resolution is characterized by the distribution of the weights appearing in the representation

$$f_\infty(x) = \sum_{i=1}^n \mathbb{E}[W_i(x; \theta)] Y_i.$$

Designs that assign non-negligible expected weight to many observations are said to have lower resolution at x , while designs that concentrate expected weight on fewer observations localized near x are said to have higher resolution at x .

Remark 3 (Interpretation). We use the term *resolution* because it more precisely characterizes the fineness of the forest’s local averaging rule and does not correspond to bias in the conventional parametric sense. Resolution describes the effective granularity of the infinite-aggregation predictor at x . Coarser weight distributions average responses over larger sets of observations, yielding increased stability across tree realizations but reduced sensitivity to local variation in the observed outcomes. Finer weight distributions concentrate mass on fewer observations, producing predictors that adapt more sharply to local structure in the realized data but that are more susceptible to dependence across trees through alignment of the induced averaging rules. All forest design parameters affect resolution through their influence on the distribution of the random weight vector $W(x; \theta)$.

5.2 Training fraction and resolution scaling

A defining feature of random forest constructions is that each tree is trained on a strict subset of the available observations. As a consequence, even under infinite aggregation the induced predictor reflects the resolution attainable by trees grown on a reduced training size. Under bootstrap resampling, the expected number of distinct observations used to construct a tree is approximately $0.632n$ (Efron, 1983). Under subsampling without replacement, the per-tree training size is fixed at $m = p_{\text{obs}} n$ for some training fraction $p_{\text{obs}} < 1$. In both cases, the distribution of the weight vector $W(x; \theta)$ depends on m , and therefore the resolution of $f_\infty(x)$ is determined by the per-tree training size rather than by the full sample size.

Although a random forest reuses observations across the ensemble, each individual tree is constructed using only $m < n$ observations. The infinite-aggregation predictor $f_\infty(x)$ is therefore an expectation over tree-level prediction rules induced by trees grown on subsamples of size m , not a prediction rule trained on all n observations. Averaging across trees combines these subsample-based predictors but does not increase the resolution beyond that attainable by the underlying tree-level fits.

Let $T_\theta^{(m)}(x)$ denote a tree constructed using m training observations, and define the corresponding infinite-aggregation target

$$f_{\infty,m}(x) = \mathbb{E}\left[T_\theta^{(m)}(x)\right].$$

Whenever the distribution of $W(x; \theta)$ varies with the per-tree training size, $f_{\infty,m}(x)$ differs from $f_{\infty,n}(x)$ for $m < n$, and this discrepancy persists as the number of trees tends to infinity. Thus, reducing the per-tree training size induces a structural reduction in resolution that cannot be compensated for by aggregation.

5.3 Structural error pathways

The strict positivity of the covariance floor established in Section 4.4 implies that, even under infinite aggregation, the forest predictor retains design-induced variability determined by the distribution of the weight vector $W(x; \theta)$. While Monte Carlo variability becomes negligible with increasing B , the structural component $C_T(x)$ reflects how the randomized design allocates weight across training observations and how these allocations co-vary across trees.

Resolution and dependence arise from different aspects of the same design-induced randomness. The infinite-aggregation predictor $f_\infty(x)$ is determined by the average weight vector $\mathbb{E}[W(x; \theta)]$, which governs the resolution of the forest at x . In contrast, the covariance floor $C_T(x)$ depends on the variability and co-movement of the random weights across design realizations. Any design choice that reduces dependence necessarily alters the distribution of these weight vectors, and therefore also affects the resolution of the infinite-aggregation predictor. This relationship is analogous to the classical bias–variance tradeoff. Structural error pathways are thus governed by how the forest design redistributes variability between resolution and dependence, rather than by Monte Carlo variance reduction alone.

6 Design parameters and their effects on resolution, dependence, and error

6.1 Parameterizing the tree-generating mechanism

We parameterize the tree-generating mechanism θ through a collection of design components defined relative to the observed sample size n . Although n is not a tuning parameter in the same sense as subsampling or split restriction, it plays a structural role by determining the support over which the induced averaging sets $A_\theta(x)$ and weight vectors $W(x; \theta)$ are defined, and therefore influences both resolution and dependence.

Each tree is generated through the following randomized steps.

1. **Observation selection.** A random index set $\mathcal{S}_\theta \subset \{1, \dots, n\}$ is drawn with fixed cardinality

$$m = |\mathcal{S}_\theta|, \quad p_{\text{obs}} = m/n,$$

defining the per-tree observation-selection fraction. The corresponding indicator vector $\mathcal{I}_\theta = (I_{\theta,1}, \dots, I_{\theta,n})$, where $I_{\theta,i} := \mathbf{1}\{i \in \mathcal{S}_\theta\}$, encodes which observations are exposed to the tree construction and governs eligibility for inclusion in the induced averaging sets $A_\theta(x)$.

2. **Split-candidate restriction.** At each internal node, a random candidate set of variables $\mathcal{J}_{\theta,v} \subset \{1, \dots, p\}$ is drawn with fixed size q . The split at that node is chosen by optimizing the splitting criterion over $\mathcal{J}_{\theta,v}$. This mechanism governs variability in the induced partitioning map M_θ and therefore controls alignment of local averaging rules across trees.
3. **Terminal occupancy constraint.** A stopping rule enforces a lower bound $s \geq 1$ on the size of the induced averaging set,

$$|A_\theta(x)| \geq s \quad \text{almost surely for all } x \text{ under consideration,}$$

ensuring that each tree-level prediction averages at least s observed outcomes. This constraint directly controls the sparsity and concentration of the weight vectors $W(x; \theta)$ and hence the effective resolution of the induced predictor.

4. **Aggregation level.** The forest predictor averages B independent realizations $\theta_1, \dots, \theta_B$. This parameter governs Monte Carlo approximation error but does not affect resolution or dependence in the infinite-aggregation limit.

The forest design is therefore characterized by the parameter vector $(n, p_{\text{obs}}, q, s, B)$. For fixed n , the parameters (p_{obs}, q, s) jointly determine the distribution of the induced averaging sets $A_\theta(x)$ and weight vectors $W(x; \theta)$, and thereby control both the resolution of the infinite-aggregation target and the dependence structure across trees. The role of B is purely to approximate this design-based target through Monte Carlo averaging.

6.2 Structural error pathways and design parameters

Sections 3 and 5 characterize how the forest design induces distinct sources of error in the finite forest predictor at a fixed prediction point x . Finite aggregation introduces Monte Carlo variability around the infinite-aggregation target, while structural dependence across trees induces a variance component that persists as the number of trees increases. The covariance decomposition in Section 4 further separates this dependence into contributions arising from shared training observations and from alignment of the induced local averaging rules.

The design parameters $(p_{\text{obs}}, q, s, B)$ act on these error pathways through distinct and interpretable mechanisms.

1. **Aggregation level (B).** The number of trees controls only the Monte Carlo component arising from finite aggregation. Increasing B improves approximation of the infinite-aggregation target $f_\infty(x)$ but does not alter the induced averaging sets $A_\theta(x)$, the distribution of weights $W(x; \theta)$, or the dependence structure across trees. Consequently, B has no effect on resolution or on the design-induced covariance floor.
2. **Training fraction (p_{obs}).** The training fraction governs which observations are exposed to each tree through the resampling indicators \mathcal{I}_θ . Increasing p_{obs} increases joint inclusion probabilities and therefore strengthens the observation-reuse component of the covariance. At the same time, it expands the support of the induced averaging sets $A_\theta(x)$, allowing finer localization and higher resolution in the infinite-aggregation target. Decreasing p_{obs} weakens dependence at the cost of coarser local averaging.
3. **Candidate-set size (q).** The number of candidate variables considered at each split governs variability in the induced partitioning map M_θ . Larger values of q increase the likelihood that similar splitting decisions are made across trees, strengthening alignment of the induced local averaging rules and increasing the alignment component of the covariance. Smaller values of q introduce additional randomness into M_θ , weakening alignment but simultaneously broadening the distribution of induced averaging sets and reducing resolution.
4. **Terminal occupancy constraint (s).** The minimum size constraint on the averaging sets $A_\theta(x)$ directly controls how concentrated the weight vectors $W(x; \theta)$ can be. Larger values of s enforce coarser local averages with greater stability but reduced resolution, while smaller values permit tighter localization around x at the cost of increased single-tree variability and stronger dependence across trees.

Together, these parameters determine how the forest design reallocates error between Monte Carlo variability, structural dependence, and resolution of the induced predictor. No choice of design parameters can simultaneously minimize all sources of error: reductions in dependence are achieved only by altering the distribution of induced averaging sets, and gains in resolution necessarily increase sensitivity to design-induced dependence.

6.3 Aggregation level B

The aggregation level B controls the number of independently generated trees averaged to form the forest predictor. Unlike the other design parameters, B does not influence how individual trees are constructed or how predictions are formed within each tree. Instead, it governs only the degree of Monte Carlo averaging applied to a fixed randomized tree-generating mechanism.

Because the forest predictor is an average of B independent realizations of the same randomized tree-level prediction rule, varying B does not alter the distribution of the underlying tree predictor $T_\theta(x)$. In particular, aggregation does not affect the induced averaging sets $A_\theta(x)$, the weight distributions $W(x; \theta)$, or any dependence arising from repeated reuse of the observed data across trees.

Remark 4 (Aggregation controls Monte Carlo variability). For any fixed tree-generating design,

$$\mathbb{E}[\hat{f}_B(x)] = f_\infty(x), \quad \text{Var}(\hat{f}_B(x)) = \frac{1}{B} \sigma_T^2(x) + \frac{B-1}{B} C_T(x).$$

Varying B therefore affects only the Monte Carlo variability arising from finite aggregation. The infinite-aggregation target $f_\infty(x)$, the single-tree dispersion $\sigma_T^2(x)$, and the design-induced covariance $C_T(x)$ are properties of the tree-generating mechanism itself and are invariant to B .

This distinction is essential for interpreting the behavior of random forests. Increasing B suppresses Monte Carlo noise around the design-induced target but cannot modify the resolution of the predictor or reduce dependence induced by the tree-generating mechanism. In particular, aggregation alone cannot eliminate the variance floor identified in Section 4.4.

6.4 Observation-selection fraction p_{obs}

The observation-selection fraction p_{obs} is a fundamental design parameter governing how much of the observed dataset is exposed to each tree. Unlike the aggregation level B , which affects only Monte Carlo averaging, p_{obs} directly alters both the dependence structure across trees and the resolution of the induced predictor.

From the perspective of dependence, p_{obs} acts exclusively through the observation-overlap component of the covariance decomposition introduced in Section 4.1 and analyzed in Section 4.2. In that representation, p_{obs} enters only through joint inclusion probabilities

$$\mathbb{P}(I_{\theta,i} = 1, I_{\theta',i} = 1),$$

which determine how frequently the same observation can receive positive weight at x in multiple trees. Increasing p_{obs} increases these joint inclusion probabilities and, holding the within-tree partitioning mechanism fixed, strengthens the observation-overlap contribution to $C_T(x)$.

Remark 5 (Monotonicity of observation-overlap dependence). Holding the partitioning mechanism fixed, the observation-overlap contribution $C_{\text{obs}}(x)$ is monotone increasing in the joint inclusion probabilities $\mathbb{P}(I_{\theta,i} = 1, I_{\theta',i} = 1)$. This follows directly from the representation in Section 4.2, where these probabilities appear as nonnegative multiplicative factors.

Independently of its effect on dependence, p_{obs} governs resolution by restricting which observations are available to define candidate splits and terminal regions. Changing the observation-selection fraction alters the induced distribution of averaging sets $A_{\theta}(x)$, equivalently the induced distribution of weights $W(x; \theta)$, and therefore changes the infinite-aggregation target $f_{\infty}(x)$. Smaller values of p_{obs} induce coarser effective averaging by limiting the amount of data available to each tree, while larger values increase resolution by averaging over prediction rules trained on larger subsets of the observed data, at the cost of stronger reuse-driven dependence across trees.

Subsampling without replacement makes this trade-off explicit. When each tree is grown on a subset of size $m = p_{\text{obs}} n$ drawn without replacement, p_{obs} becomes a tunable design parameter that directly controls both resolution and dependence. Decreasing p_{obs} weakens observation reuse across trees but reduces the resolution attainable by the induced predictor; increasing p_{obs} improves resolution while strengthening dependence through repeated reuse of the same observations.

The bootstrap corresponds to a particular, non-tunable choice of p_{obs} . Although each tree is grown from a resample of size n , the expected fraction of distinct observations exposed to the tree satisfies

$$\mathbb{P}(i \in \mathcal{I}_{\theta}) = 1 - (1 - 1/n)^n \approx 1 - e^{-1}, \quad \mathbb{P}(i \in \mathcal{I}_{\theta} \cap \mathcal{I}_{\theta'}) \approx (1 - e^{-1})^2.$$

Thus, under bootstrap resampling the observation-selection fraction is implicitly fixed by the resampling scheme, and the resulting magnitude of observation-induced dependence is an intrinsic feature of the design rather than a tunable choice.

From a design-based perspective, subsampling without replacement reveals that observation selection is not merely an implementation detail but a central mechanism through which random forests trade resolution against structural dependence.

6.5 Split-candidate restriction size q

Restricting the number of candidate variables considered at each split alters the dependence structure of the forest by changing how frequently independently generated trees induce the same local prediction rule at a prediction point x . This effect operates through alignment of the induced local averaging rules at x , as discussed in Section 4.3. In particular, restricting candidate variables reduces the opportunity for identical early split decisions along the path to x , thereby weakening alignment-induced dependence across trees.

Let $q \in \{1, \dots, p\}$ denote the number of candidate variables sampled at each internal node. Decreasing q reduces the amount of shared candidate information available across trees at each split, which in turn reduces the probability that two trees make identical split decisions along the path to x . Here, two prediction rules are said to be identical at x if they induce the same resampling-conditional weight vector $\bar{W}(x; \mathcal{I})$, equivalently if they define the same local averaging rule at x after averaging over split-level randomization.

This mechanism can be made explicit through a simple combinatorial property of random subspace selection.

Lemma 1 (Shared candidate variables under random subspaces). *Fix an internal node v . Under uniform sampling without replacement of candidate sets of size q at node v ,*

$$\mathbb{E}\left[\left|S_{\theta,v}^{(q)} \cap S_{\theta',v}^{(q)}\right|\right] = \frac{q^2}{p},$$

where $S_{\theta,v}^{(q)}$ and $S_{\theta',v}^{(q)}$ denote the candidate-variable sets drawn independently for two trees. In particular, the expected overlap is strictly increasing in q for $q \in \{1, \dots, p\}$.

Lemma 1 does not assert that trees select the same splits, but isolates the design mechanism by which candidate restriction controls the opportunity for repeated split selection across trees. Whether this opportunity translates into actual alignment depends on the stability of split selection, which is addressed by the following result.

Proposition 2 (Candidate restriction weakens alignment probability). *Fix a prediction point x . Consider two forest designs that differ only in candidate-set size, with $q' < q$. Define the alignment probability under candidate-set size q as*

$$\alpha_q(x) := \mathbb{P}\left(Z_{\theta}^{(q)}(x) = Z_{\theta'}^{(q)}(x)\right),$$

where $Z_{\theta}^{(q)}(x) = \mathbb{E}[T_{\theta}^{(q)}(x) \mid \mathcal{I}_{\theta}]$ denotes the resampling-conditional prediction rule under candidate-set size q , and θ, θ' are independent draws from the tree-generating mechanism. Assume that at each internal node along the path to x , the splitting criterion has a unique maximizer over the candidate set almost surely. Then

$$\alpha_{q'}(x) \leq \alpha_q(x),$$

with strict inequality whenever restricting from q to q' alters split selection with positive probability along the path to x .

Proposition 2 formalizes the role of candidate restriction as a mechanism for weakening alignment-induced dependence. Reducing q decreases the probability that independently generated trees induce identical local averaging rules at x , thereby reducing the alignment component of the structural covariance.

Candidate restriction also affects the induced predictor itself through its impact on the distribution of local averaging rules. Because the infinite-aggregation predictor $f_{\infty}(x)$ is fully determined by the distribution of the resampling-conditional prediction rule $Z_{\theta}(x)$, any change in candidate-set size that alters this distribution necessarily alters the induced predictor.

Remark 6 (Effect of candidate restriction on the induced predictor). The infinite-aggregation predictor $f_\infty(x)$ is the expectation of the prediction rule $Z_\theta(x)$. If two designs induce different distributions of $Z_\theta(x)$, their expectations differ unless $Z_\theta(x)$ is almost surely constant, which occurs only in degenerate cases. Consequently, changes in q that alter the distribution of $Z_\theta(x)$ necessarily alter the induced predictor.

Resolution at x is governed by the average weight vector $\mathbb{E}[W(x; \theta)]$, which depends on the distribution of the resampling-conditional prediction rule $Z_\theta(x)$. Increasing q enlarges the shared candidate information across trees, concentrating the distribution of induced local averaging rules and reducing variability in split selection along the path to x . Conversely, decreasing q increases heterogeneity in the induced neighborhoods and broadens the distribution of weight vectors. Thus, larger q produces a more stable and concentrated resolution structure, while smaller q increases diversity of local averaging behavior.

In contrast, reducing q weakens alignment and decreases alignment-induced dependence, while simultaneously increasing randomness in the induced local averaging rules through greater variability in split selection. Candidate restriction redistributes structure between dependence and diversity of local averaging behavior, rather than eliminating either source of structure, and is central to the practical success of random forests.

6.6 Minimum terminal occupancy s

The minimum terminal occupancy parameter s governs the spatial resolution of the tree-level prediction rules by imposing a lower bound on the number of observations contained in each terminal region. Larger values of s enforce coarser partitions by preventing further splitting once terminal regions contain fewer than s observations, while smaller values permit continued splitting and therefore finer localization around the prediction point x . Because the infinite-aggregation predictor $f_\infty(x)$ is determined by the distribution of terminal regions (equivalently, by the induced distribution of weight vectors), changes in s act by modifying the scale at which local averaging is performed.

Increasing s enlarges the terminal regions used to form predictions, producing coarser local averaging behavior and reduced sensitivity to fine-scale variation in the observed outcomes. Decreasing s permits smaller terminal regions and therefore higher-resolution predictors that adapt more sharply to local features of the realized data. This effect is structural: even under infinite aggregation, the induced predictor reflects the resolution attainable by trees grown subject to the terminal-occupancy constraint.

The same mechanism also affects variability and dependence across trees. Smaller terminal regions average fewer observations, which increases sensitivity to local outcome variation and raises the marginal dispersion of individual tree predictions. Larger values of s stabilize individual trees by enforcing broader averaging, but simultaneously promote reuse of similar coarse partitions across tree realizations. This increased regularity strengthens alignment of induced local averaging rules and can therefore increase structural dependence across trees.

Proposition 3 (Terminal occupancy and local resolution). *Consider two forest designs that differ only in the minimum terminal occupancy, with $s' < s$. Under the monotone-growth assumption, reducing s shifts the distribution of terminal regions at x toward smaller local averaging sets.*

Proposition 3 formalizes the role of the terminal-occupancy constraint as a resolution parameter. Lowering s allows finer partitioning near x , while increasing s enforces coarser averaging that persists under infinite aggregation. The proof relies only on the structural nesting of partitions induced by monotone tree growth and does not require distributional assumptions on the outcomes.

6.7 Sample size and persistence of structural dependence

This subsection addresses whether increasing sample size alone can eliminate structural dependence across trees when such dependence is induced by the tree-generating design. Throughout, the design parameters (p_{obs}, q, s) are held fixed as n varies.

Write

$$f_{\infty, n}(x) = \mathbb{E}[T_{\theta}^{(n)}(x)], \quad C_{T, n}(x) = \text{Cov}\left(T_{\theta}^{(n)}(x), T_{\theta'}^{(n)}(x)\right),$$

where $T_{\theta}^{(n)}$ denotes a tree grown on a dataset of size n under the same randomized construction.

Existing large-sample analyses of random forests describe how increasing n refines the induced partitions and improves the resolution of the infinite-aggregation predictor. These results concern how the local averaging behavior at x evolves with additional data, but they do not address whether dependence between independently generated trees weakens as the sample size grows.

From the finite-sample covariance decomposition, $C_{T, n}(x)$ is governed by the joint distribution of resampling patterns and induced local averaging rules. Increasing n refines these rules but does not alter the sources of randomization in the tree-generating mechanism. In particular, when split selection along the path to x remains randomized—due to candidate restriction, enforced terminal occupancy, or non-unique split choices—the distribution of local prediction rules does not collapse to a single deterministic rule.

Consequently, increasing sample size alone does not remove design-induced dependence across trees. Any reduction in structural covariance must arise from changes to the design itself, not from refinement of partitions driven by larger n .

6.8 Why added randomization improves finite-sample behavior

Additional randomization in split selection is a design parameter that directly alters the dependence structure of the forest and the distribution of induced local prediction rules. Unlike aggregation, which averages independent realizations of a fixed randomized procedure, added randomization modifies the tree-generating mechanism itself and therefore changes both the induced predictor and its structural dependence properties.

A concrete example is augmented bagging, which introduces $r \geq 0$ independent noise variables into the predictor space prior to growing each tree, making r an explicit randomization parameter (Mentch and Zhou, 2022). Increasing r reduces the probability that any particular split is repeatedly selected along the path to a prediction point x , thereby dispersing the distribution of local decision rules induced by the forest design.

From the perspective developed in Section 4.3, this dispersion weakens alignment of induced prediction rules across trees. When randomization is weak, the tree-generating mechanism can concentrate probability on a small family of local averaging rules at x , leading independently generated trees to repeatedly induce similar neighborhoods and hence strong alignment-induced dependence. Increasing the level of randomization reduces this concentration by lowering the chance that the same early split decisions recur across trees, thereby weakening alignment and reducing the corresponding contribution to structural dependence.

At the same time, added randomization necessarily alters the distribution of induced partitions and local averaging behavior. By spreading probability mass across a broader collection of admissible decision rules, increased randomization modifies the resolution of the induced predictor at x . Local averaging behavior becomes more diverse across tree realizations, reflecting greater variability in how observations are grouped with x under the design.

These two effects act in opposition. Added randomization weakens alignment and reduces structural dependence across trees, while simultaneously redistributing probability mass across local prediction rules and altering resolution. Improvements in finite-sample behavior arise when the reduction in alignment-induced dependence outweighs the accompanying change in resolution. This trade-off is inherently finite-sample: increasing the number of trees suppresses Monte Carlo variability but does not modify the design-induced structure that governs alignment and resolution.

This perspective unifies several existing explanations for the empirical benefits of randomization in tree ensembles. Augmented bagging demonstrates that deliberately increasing randomness at the tree level can improve ensemble performance by weakening dependence across trees (Mentch and Zhou, 2022). Related analyses interpret this behavior through regularization effects (Mentch and Zhou, 2020), performance gains in randomized tree constructions (Liu and Mazumder, 2025), or smoothing properties of forests controlled by design parameters (Curth et al., 2024). The present framework makes these effects explicit at a fixed prediction point x by identifying alignment-induced dependence and resolution as the two competing design-driven mechanisms through which added randomization acts.

7 Discussion

This paper develops a finite-sample, design-based characterization of random forest predictors by treating each tree as a randomized prediction rule acting on fixed data. Under this formulation, all randomness arises from the tree-generating mechanism, and prediction variability is governed by the induced distribution of terminal regions and associated weights. The resulting framework establishes random forests as explicit statistical procedures whose behavior can be analyzed through the same conditioning logic used in classical design-based inference.

A key motivation for this perspective is that random forests differ fundamentally from deterministic prediction procedures. For linear or generalized linear models, the prediction at a fixed point x is an algebraic function of the observed data, and variability arises exclusively from sampling. In random forests, the prediction depends on both the data and the procedural randomization θ , introducing a design-induced variability component that has no analogue in deterministic methods. This additional component decomposes into Monte Carlo noise, which diminishes under sufficient aggregation, and a structural covariance floor $C_T(x)$, which does not. The covariance floor is a cost of randomization, paid in exchange for the benefits of ensemble diversity and the ability to trade resolution against stability through hyper-parameters.

The exact variance identity in Theorem 1 makes this separation precise. The Monte Carlo component $\sigma_T^2(x)/B$ governs seed-to-seed variability and goes to zero as B grows, while $C_T(x)$ remains as the irreducible variance floor under infinite aggregation. Decomposing $C_T(x)$ via the law of total covariance reveals two structurally distinct mechanisms: observation reuse, whereby shared training outcomes induce correlated predictions, and partition alignment, whereby independently generated trees discover similar local geometry near x and define similar averaging rules even when their training data are disjoint. These mechanisms operate through different features of the tree-generating process and respond to different design parameters – observation reuse to the training fraction p_{obs} , and alignment to the candidate-set size q and the level of split-level randomization.

These results carry direct practical implications. Stabilization of forest predictions across random seeds for tree generation – a standard assessment of sufficient aggregation – reflects only the elimination of the Monte Carlo component and does not indicate the absence or magnitude of $C_T(x)$. A forest whose predictions no longer vary across constructions has converged to its infinite-aggregation target $f_\infty(x)$, but the precision of that target is governed by the structural covariance between trees. This covariance floor is not detectable through repeated forest construction at fixed B ; it is a property of the dependence structure among tree-level predictions and can only be assessed by examining their joint behavior within a single forest.

More broadly, existing asymptotic confidence intervals for random forest predictions, including those based on U-statistic and influence-function representations (Mentch and Hooker, 2016; Wager and Athey, 2018), target the sampling variability of the infinite-aggregation functional $f_\infty(x)$ under repeated data generation. That is, they quantify how $f_\infty(x)$ would vary across new datasets drawn from the same population. Within this sampling-based estimand, these procedures are correctly calibrated. However, they do not incorporate the additional design-induced variability captured by $C_T(x)$, which reflects dependence among

trees within a fixed dataset and persists under infinite aggregation at fixed sample size. The sampling component decreases at rate $O(n^{-1})$, while $C_T(x)$ at fixed design parameters does not necessarily decay at the same rate. When $C_T(x)$ is non-negligible relative to the sampling variance, intervals based solely on asymptotic sampling theory quantify sampling uncertainty but may not reflect the total predictive variability of the finite-sample forest procedure.

Within this framework, the effect of added randomization admits a precise finite-sample explanation. Additional randomization disperses the distribution of induced partitions, weakening alignment across trees and reducing the corresponding contribution to $C_T(x)$, while simultaneously altering the resolution of the induced predictor. Finite-sample improvements arise when the reduction in alignment-induced dependence outweighs the accompanying change in resolution. This mechanism follows directly from the variance identity and the covariance decomposition, without appeal to asymptotic arguments or heuristic notions of regularization. The framework thereby unifies several existing explanations for the empirical benefits of randomization in tree ensembles (Mentch and Zhou, 2020, 2022; Liu and Mazumder, 2025; Curth et al., 2024) by identifying alignment-induced dependence and resolution as the two competing design-driven mechanisms through which added randomization acts.

The present framework complements the existing theoretical literature on random forests. Prior work has established consistency, convergence rates, and asymptotic distributions under increasing sample size, typically by representing forests as weighted nearest-neighbor or U-statistic-type estimators. These results characterize sampling variability but do not isolate the finite-sample dependence induced by the tree-generating mechanism at fixed data. By conditioning on the observed dataset and analyzing the design-induced distribution, the present approach identifies the structural sources of dependence that govern finite-sample behavior and persist under aggregation. Within this formulation, the object of study is the random forest predictor itself, in the same sense that one studies the properties of a fitted generalized linear model independently of how cross-validation is used to assess its performance. Out-of-bag predictions and related resampling-based performance estimates correspond to distinct estimands and should not be conflated with the predictor. Understanding how such estimators inherit and interact with the structural dependence identified here is a natural direction for future work. The covariance floor $C_T(x)$ is itself directly estimable from the sample covariance of tree-level predictions within a fitted forest, since these predictions are exchangeable under the design distribution. Decomposing $C_T(x)$ into its overlap and alignment components, however, requires the conditional variance quantities σ_i^2 , which are properties of the data-generating process rather than the randomized design. Developing estimators for these individual components, together with their finite-sample properties, is deferred to subsequent work.

8 Conclusion

This paper develops a finite-sample, design-based characterization of random forest predictors by viewing each tree as a randomized tree-level prediction rule acting on fixed data. Conditioning on the design yields an exact variance identity that separates aggregation variability from structural dependence induced by the tree-generating mechanism and decomposes this dependence into observation-overlap and partition-alignment components. This framework clarifies the role of randomization in controlling finite-sample prediction variability by weakening structural dependence and reshaping resolution, and provides a principled basis for understanding how forest design parameters govern ensemble behavior beyond aggregation effects alone.

References

Susan Athey, Julie Tibshirani, and Stefan Wager. Generalized random forests. *The Annals of Statistics*, 47(2):1148–1178, 2019.

Gérard Biau. Analysis of a random forests model. *Journal of Machine Learning Research*, 13:1063–1095, 2012.

Gérard Biau and Luc Devroye. On the layered nearest neighbour estimate, the bagged nearest neighbour estimate and the random forest method in regression and classification. *Journal of Multivariate Analysis*, 101(10):2499–2518, 2010.

Gérard Biau and Erwan Scornet. A random forest guided tour. *Test*, 25:197–227, 2016.

Gérard Biau, Luc Devroye, and Gábor Lugosi. Consistency of random forests and other averaging classifiers. *Journal of Machine Learning Research*, 9:2015–2033, 2008.

Leo Breiman. Bagging predictors. *Machine Learning*, 24:123–140, 1996.

Leo Breiman. Random forests. *Machine Learning*, 45(1):5–32, 2001.

Leo Breiman. Consistency for a simple model of random forests. Technical report, University of California, Berkeley, 2004.

Leo Breiman, Jerome Friedman, Richard Olshen, and Charles Stone. *Classification and Regression Trees*. Wadsworth, 1984.

Gavin Brown, Jeremy Wyatt, Rachel Harris, and Xin Yao. Diversity creation methods: A survey and categorisation. *Information Fusion*, 6:5–20, 2005.

Peter Bühlmann and Bin Yu. Analyzing bagging. *The Annals of Statistics*, 30(4):927–961, 2002.

Alicia Curth, Alan Jeffares, and Mihaela van der Schaar. Why do random forests work? understanding tree ensembles as self-regularizing adaptive smoothers, 2024. URL <https://arxiv.org/abs/2402.01502>.

Thomas Dietterich. Ensemble methods in machine learning. *Multiple Classifier Systems*, pages 1–15, 2000.

Bradley Efron. Estimating the error rate of a prediction rule. *Journal of the American Statistical Association*, 78(382):316–331, 1983.

Trevor Hastie, Robert Tibshirani, and Jerome Friedman. *The Elements of Statistical Learning*. Springer, 2009.

Tin Kam Ho. The random subspace method for constructing decision forests. *IEEE Transactions on Pattern Analysis and Machine Intelligence*, 20(8):832–844, 1998.

Ludmila Kuncheva and Christopher Whitaker. Measures of diversity in classifier ensembles. *Machine Learning*, 51:181–207, 2003.

Yi Lin and Yongho Jeon. Random forests and adaptive nearest neighbors. *Journal of the American Statistical Association*, 101(474):578–590, 2006.

Brian Liu and Rahul Mazumder. Randomization can reduce bias and variance of decision trees. *Journal of Machine Learning Research*, 26(150):1–49, 2025.

Miles E. Lopes, Suofei Wu, and Thomas Lee. Measuring the algorithmic convergence of randomized ensembles: The regression setting. *arXiv preprint arXiv:1908.01251*, 2019a.

Miles E. Lopes, Suofei Wu, and Thomas Lee. Estimating the algorithmic variance of randomized ensembles via the bootstrap. *The Annals of Statistics*, 47(2):1088–1112, 2019b.

Nicolai Meinshausen. Quantile regression forests. *Journal of Machine Learning Research*, 7:983–999, 2006.

Lucas Mentch and Giles Hooker. Quantifying uncertainty in random forests via confidence intervals and hypothesis tests. *Journal of Machine Learning Research*, 17(26):1–41, 2016.

Lucas Mentch and Siyu Zhou. Randomization as regularization: A degrees of freedom explanation for random forest success. *Journal of Machine Learning Research*, 21(171):1–36, 2020.

Lucas Mentch and Siyu Zhou. Getting better from worse: Augmented bagging and a cautionary tale of variable importance. *Journal of Machine Learning Research*, 23(224):1–32, 2022.

Erwan Scornet, Gérard Biau, and Jean-Philippe Vert. Consistency of random forests. *The Annals of Statistics*, 43(4):1716–1741, 2015.

Stefan Wager and Susan Athey. Estimation and inference of heterogeneous treatment effects using random forests. *Journal of the American Statistical Association*, 113(523):1228–1242, 2018.

Tianning Xu, Ruqing Zhu, and Xiaofeng Shao. On variance estimation of random forests with infinite-order u-statistics. *Electronic Journal of Statistics*, 18(1):2135–2207, 2024.

Zhengze Zhou, Lucas Mentch, and Giles Hooker. V-statistics and variance estimation. *Journal of Machine Learning Research*, 22(287):1–48, 2021.

A Sampling variability of the infinite-forest target

This appendix establishes that the sampling variability of the infinite-aggregation random forest target is generically of order n^{-1} under standard stability conditions.

Let $\mathcal{D}_n^* = \{Z_i = (X_i, Y_i)\}_{i=1}^n$ denote an i.i.d. sample from an underlying population, and define the infinite-aggregation forest functional

$$f_\infty(x; \mathcal{D}) = \mathbb{E}_\Theta [\hat{f}_B(x; \mathcal{D}, \theta)].$$

Assume that $f_\infty(x; \mathcal{D}_n^*)$ admits an asymptotically linear expansion of the form

$$f_\infty(x; \mathcal{D}_n^*) = f(x) + \frac{1}{n} \sum_{i=1}^n \psi_x(Z_i) + r_n(x),$$

where $\mathbb{E}[\psi_x(Z_i)] = 0$, $\mathbb{E}[\psi_x(Z_i)^2] < \infty$, and $\sqrt{n} r_n(x) \rightarrow 0$ in L^2 .

Taking variances yields

$$\text{Var}(f_\infty(x; \mathcal{D}_n^*)) = \text{Var}\left(\frac{1}{n} \sum_{i=1}^n \psi_x(Z_i)\right) + \text{Var}(r_n(x)) + 2 \text{Cov}\left(\frac{1}{n} \sum_{i=1}^n \psi_x(Z_i), r_n(x)\right).$$

By independence and finite second moment,

$$\text{Var}\left(\frac{1}{n} \sum_{i=1}^n \psi_x(Z_i)\right) = \frac{\text{Var}(\psi_x(Z_1))}{n}.$$

The remainder terms satisfy $\text{Var}(r_n(x)) = o(n^{-1})$ and $\text{Cov}(n^{-1} \sum_i \psi_x(Z_i), r_n(x)) = o(n^{-1})$ by the assumed L^2 rate.

Consequently,

$$\text{Var}(f_\infty(x; \mathcal{D}_n^*)) = \frac{\text{Var}(\psi_x(Z_1))}{n} + o(n^{-1}),$$

so the sampling variability of the infinite-forest target is generically of order n^{-1} .

Such asymptotic linear representations and variance calculations are standard for stable estimators; see Mentch and Hooker (2016) and Wager and Athey (2018) for applications to random forest-type procedures.

B Proof of Lemma 1

Proof. Fix a realized dataset \mathcal{D}_n and a node index v . All probability statements are taken with respect to the tree-generating randomization. For each tree θ , let $S_{\theta, v}^{(m)} \subset \{1, \dots, p\}$ denote the candidate variable set drawn at node v under candidate-set size m .

We construct a coupling across values of m as follows. For each tree θ and node v , draw an independent uniform random permutation $\pi_{\theta, v}$ of $\{1, \dots, p\}$, and define

$$S_{\theta, v}^{(m)} = \{\pi_{\theta, v}(1), \dots, \pi_{\theta, v}(m)\}.$$

This construction yields the correct marginal distribution for uniform sampling without replacement of size- m candidate sets.

Under this coupling, for any $m_1 < m_2$,

$$S_{\theta, v}^{(m_1)} \subset S_{\theta, v}^{(m_2)}, \quad S_{\theta', v}^{(m_1)} \subset S_{\theta', v}^{(m_2)}.$$

Since $\pi_{\theta,v}$ and $\pi_{\theta',v}$ are independent, the intersection size

$$|S_{\theta,v}^{(m)} \cap S_{\theta',v}^{(m)}|$$

follows a hypergeometric distribution with expectation

$$\mathbb{E}[|S_{\theta,v}^{(m)} \cap S_{\theta',v}^{(m)}|] = \frac{m^2}{p}.$$

This expectation is strictly increasing in m for $m \in \{1, \dots, p\}$, establishing the claimed monotonicity of candidate-set overlap. \square

C Proof of Theorem 2

Proof. Fix a prediction point x and a realized dataset $\mathcal{D}_n = \{(X_i, Y_i)\}_{i=1}^n$. All expectations and covariances are taken with respect to the tree-generating randomization.

Design-based second-moment convention. The quantities $\sigma_i^2 = \text{Var}(Y_i \mid X_i)$ are treated as fixed conditional second moments evaluated at the observed covariate values and enter the covariance expansion only as scaling factors.

Step 1: A nonnegative lower bound for $C_T(x)$. By the law-of-total-covariance decomposition in (3),

$$C_T(x) = \mathbb{E}[\text{Cov}(T_\theta(x), T_{\theta'}(x) \mid \mathcal{I}_\theta, \mathcal{I}_{\theta'})] + \text{Cov}(\mathbb{E}[T_\theta(x) \mid \mathcal{I}_\theta], \mathbb{E}[T_{\theta'}(x) \mid \mathcal{I}_{\theta'}]).$$

In particular,

$$C_T(x) \geq \mathbb{E}[\text{Cov}(T_\theta(x), T_{\theta'}(x) \mid \mathcal{I}_\theta, \mathcal{I}_{\theta'})].$$

Step 2: Strict positivity of the observation-reuse contribution. Under conditional independence across observational units given the fixed design points, Section 4.2 shows that

$$\mathbb{E}[\text{Cov}(T_\theta(x), T_{\theta'}(x) \mid \mathcal{I}_\theta, \mathcal{I}_{\theta'})] = \sum_{i=1}^n \sigma_i^2 \mathbb{E}[W_i(x; \theta) W_i(x; \theta')],$$

a sum of nonnegative terms.

By assumption, there exists i^* such that $\sigma_{i^*}^2 > 0$ and $\mathbb{P}(W_{i^*}(x; \theta) > 0) > 0$. Independence of θ and θ' implies

$$\mathbb{P}(W_{i^*}(x; \theta) > 0, W_{i^*}(x; \theta') > 0) = \mathbb{P}(W_{i^*}(x; \theta) > 0)^2 > 0.$$

On this event, $W_{i^*}(x; \theta) W_{i^*}(x; \theta') > 0$, and therefore

$$\mathbb{E}[W_{i^*}(x; \theta) W_{i^*}(x; \theta')] > 0.$$

Hence the i^* summand is strictly positive, and the entire sum is strictly positive.

Step 3: Conclusion. Combining Step 1 and Step 2 yields $C_T(x) > 0$. The limit statement follows from Theorem 1, since $\lim_{B \rightarrow \infty} \text{Var}(\hat{f}_B(x)) = C_T(x)$. \square

D Proof of Proposition 2

Fix a prediction point x . Consider two forest designs that differ only in the candidate-set size at each split, with $q' < q$. Let

$$Z_\theta^{(q)}(x) = \mathbb{E}[T_\theta^{(q)}(x) | \mathcal{I}_\theta], \quad Z_\theta^{(q')}(x) = \mathbb{E}[T_\theta^{(q')}(x) | \mathcal{I}_\theta]$$

denote the corresponding resampling-conditional prediction rules.

We construct the two designs on a common probability space as follows. At each internal node, the candidate set under the q' -design is obtained by subsampling without replacement from the candidate set under the q -design. All remaining sources of randomness (observation selection, split-point evaluation, and tie-breaking) are shared across designs. This coupling is conceptual and used only for comparison of induced rule distributions; it does not correspond to an implemented algorithm.

Along the path to x , the q -design evaluates splits over a superset of coordinates relative to the q' -design. Consequently, whenever the q' -design selects a particular split at a node, the q -design either selects the same split or selects a different split only if an additional candidate variable available under q yields a strictly better value of the splitting criterion. Under the stated nondegeneracy conditions, ties occur with probability zero or are resolved identically.

Therefore, whenever two independent trees generated under the q' -design induce identical conditional prediction rules at x , the corresponding trees under the q -design also induce identical conditional prediction rules. Writing

$$A_q(x) = \{Z_\theta^{(q)}(x) = Z_{\theta'}^{(q)}(x)\}, \quad A_{q'}(x) = \{Z_\theta^{(q')}(x) = Z_{\theta'}^{(q')}(x)\},$$

this implies

$$A_{q'}(x) \subseteq A_q(x) \quad \text{with probability one under the coupling.}$$

Taking probabilities yields $\alpha_{q'}(x) \leq \alpha_q(x)$. If restricting from q to q' alters the selected split with positive probability along the path to x , then the inclusion is strict on an event of positive probability, implying $\alpha_{q'}(x) < \alpha_q(x)$. \square

E Proof of Proposition 3

Assumption (monotone tree growth in s). Trees grown under different minimum-terminal-occupancy constraints can be constructed on a common probability space such that, for fixed underlying randomization (observation selection, candidate restriction, and tie-breaking), the partition generated under $s' < s$ is a refinement of the partition generated under s . Along every root-to-leaf path, the s' -tree performs all splits performed by the s -tree and possibly additional splits, and it never reverses an earlier split.

Proof. Fix a prediction point x and construct two trees $\theta^{(s)}$ and $\theta^{(s')}$ on the same probability space satisfying the monotone-growth assumption. By refinement,

$$\mathcal{R}_{\theta^{(s')}}(x) \subseteq \mathcal{R}_{\theta^{(s)}}(x) \quad \text{almost surely.}$$

Because terminal-region size is defined by the number of observations contained in the region,

$$|\mathcal{R}_{\theta^{(s')}}(x)| \leq |\mathcal{R}_{\theta^{(s)}}(x)| \quad \text{almost surely.}$$

Taking expectations yields

$$\mathbb{E}[|\mathcal{R}_{\theta^{(s')}}(x)|] \leq \mathbb{E}[|\mathcal{R}_{\theta^{(s)}}(x)|].$$

This establishes that reducing s shifts probability mass toward smaller terminal regions at x and therefore induces finer local averaging behavior. \square